Autocatalytic Oxidation of Cyclohexane—Mass Transfer and Chemical Reaction

In an industrial gas-liquid reactor both mass transfer and kinetics have, in principle, a role to play. This paper describes studies on the oxidation of cyclohexane in two-phase, gas-liquid reactors. Regimes of absorption have been clarified by measurements of dissolved oxygen concentrations. The behavior is found to be complex, arising from the fact that the reaction is autocatalytic, and zero order in oxygen over almost the entire absorption range. As reaction velocity increases, due to the autocatalytic kinetics, enhanced physical mass transfer rates arise. Bubble swarms have properties that prevent the simple application of mass transfer and enhancement from flat-surface systems. A theory is developed here that accounts qualitatively for the enhancement found in bubble swarms in the present case. The theory is also shown to predict quantitatively the appropriate physical mass transfer coefficients.

A. K. Suresh, T. Sridhar, O. E. Potter
Department of Chemical Engineering
Monash University
Clayton, Victoria 3168, Australia

Introduction

In an industrial gas-liquid oxidation reactor, both mass transfer and kinetics have a role to play, since the oxygen from the gas phase has to be transported to the site of reaction in the liquid. This paper describes studies on the oxidation of cyclohexane in two-phase (gas-liquid) reactors. In such studies, proper interpretation of the absorption rates relies crucially on establishing the regime of absorption. The measurement of the dissolved gas concentration during reaction provides a direct means of doing this and has been used in the present work to identify the absorption regimes. Such a procedure avoids the pitfalls in estimating the relative rates of mass transfer and chemical reaction through correlations (of sometimes dubious accuracy). The reactors used in the experimental studies have been described by Suresh et al. (1987a). In particular, the sparged and agitated stirred-tank reactor is in many ways representative of the contacting conditions in an industrial oxidation reactor. This paper describes the general features of a batch oxidation in the gas-liquid mode, such that in the one experiment the system is initially kinetically controlled and then becomes controlled by physical mass transfer, and may then become controlled by enhancement of mass transfer due to chemical reaction in the film.

A. K. Suresh is presently with Hindusthan Lever Research Center, Bombay, India.

Experimental Procedure

The stirred-tank reactor (STR) and the flat interface reactor (FIR), their operating procedures, and the associated monitoring systems and analysis procedures have been detailed by Suresh et al. (1987a). An operating pressure of 12–13 bar was used in all the experiments. The usual start-up procedure was to establish steady conditions of temperature, pressure, and liquid level with nitrogen flowing through the equipment at the required superficial velocity, and then change over to the appropriate oxygen-nitrogen mixture. Different inlet oxygen levels were used in the STR, while a premixed gas mixture containing 4% oxygen in nitrogen was used in all the experiments in the FIR. The course of the reaction was followed by continuously monitoring the oxygen content in the gases leaving the reactor (in the STR, the oxygen content of the exhaust gases was also continuously followed to provide a second check on the absorption rates) and by determining the dissolved oxygen concentration in the reactor as a function of time. Samples were withdrawn from the reactor and stored. The reactor temperature was continuously recorded and the reactor level and the stirrer speed were maintained constant throughout the experiments.

Analytical grade cyclohexane was used in all the experiments. The induction periods proved difficult to reproduce exactly unless the reactors were physically taken apart and thoroughly cleaned. Fortunately, the need for this did not arise too frequently, since an exact reproduction of the induction period was not

critical. Different induction periods only meant that the different experiments could not be compared on the basis of batch time. They could, however, be compared on the basis of conversions.

The absorption rates in the sparged reactor were measured at the exit of the reactor as well as at the exhaust (using oxygen probes), and also checked from time to time by analyzing the gases leaving the reactor for oxygen on a gas chromatograph fitted with an electron capture detector. The oxygen measurements at the exhaust had to be corrected for time lags, in view of the considerable volume between the reactor and the sampling point and the time-varying nature of the absorption rates in this system. The three determinations usually gave results close to each other, as shown by Figure 1. The agreement between the rates measured, at the exit of the reactor and at the exhaust, shows that reaction downstream of the reactor is negligible.

General Features of the Batch Oxidation

Since the reaction is one that starts off at almost zero velocity (during the induction period) and speeds up with time as the reaction products accumulate, one might in general expect the absorption rates also to vary in the same manner. The general features of a batch oxidation, under the conditions of high mass transfer rates that typically obtain in bubbling agitated contactors, are best illustrated by the results of a typical experiment at 423 K in the STR. Figure 1 shows the absorption rate and dissolved oxygen concentrations measured during an experiment carried out in the STR with 2.9% oxygen at the reactor inlet. Immediately after oxygen is admitted into the reactor, there is a brief period (about 0.5 min) of physical absorption during which the dissolved oxygen concentration increases and absorption rate decreases (this period is not shown in the figure). Absorption ceases when the liquid becomes saturated with oxygen at the prevailing partial pressure. Then follows the induction period, with the liquid remaining saturated and the absorption rate

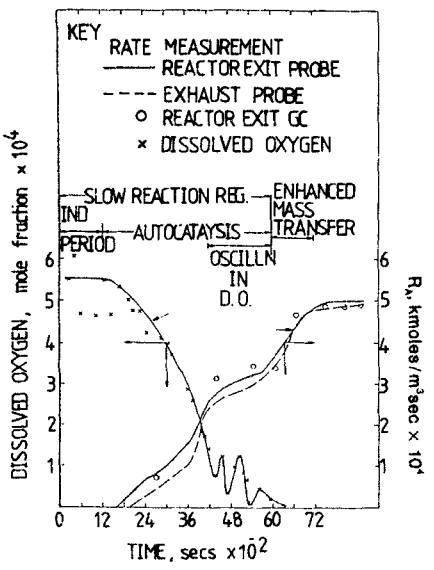

Figure 1. Variation of dissolved oxygen and absorption rate in a stirred-tank reactor at 423 K.

p_o = 0.36 bar; $U_G = 0.92 \times 10^{-2}$ m/s; RPS = 16.1

being too small to be measurable. Induction periods at 423 K were typically of about 20–30 min duration. As the free radicals accumulate, the reaction velocity begins to increase and this is indicated by decreasing dissolved oxygen concentrations and increasing absorption rates. This is the slow reaction regime, with the reaction not being fast enough to take place appreciably in the diffusion film, and virtually all the oxygen that is absorbed getting through the bulk of the liquid. Due to autocatalysis, the absorption rate increases continuously with time, and to accommodate the increasing absorption rates, the dissolved oxygen concentration decreases, as shown by the data in Figure 1, ultimately falling to negligible levels. The rate of oxygen absorption increases more slowly than before as the dissolved oxygen concentration approaches zero and shows a tendency to become diffusion-limited. Hydrocarbon oxidations, which are normally zero order in oxygen, are expected to become first order in oxygen at sufficiently small oxygen levels, and the tail in the dissolved oxygen curve as it approaches zero asymptotically is indicative of such a transition. In a number of cases, the dissolved oxygen concentration showed a tendency to oscillate in this region before ultimately decreasing to zero. At larger times, depending on the oxygen partial pressure, the contacting conditions, and the temperature, a second period of increasing absorption rate was sometimes observed.

Not all the experiments exhibited all the features shown in Figure 1. For example, in the experiments at 413 K, the concentration of dissolved oxygen in the bulk did not decrease to zero, because of the smaller kinetic rates. At 423 K, the region of mass transfer enhancements was only observed when the partial pressures were low.

Since the fact that the dissolved oxygen concentration decreases to zero must mean that mass transfer can no longer keep up with the intrinsic reaction rate beyond a certain conversion, the absorption data at higher conversions should be considered to be influenced by mass transfer limitations. One cannot, therefore, realize true kinetic rates when the dissolved oxygen analysis shows zero oxygen in the bulk liquid. Thus again, the measurement of dissolved oxygen concentrations provides direct evidence for the existence of mass transfer limitations.

With the dissolved oxygen at negligible levels, the mass transfer coefficient can be calculated from the rate of absorption and the partial pressure of oxygen at the exit of the reactor, if the gas and liquid phases can be assumed to be well mixed. The volumetric mass transfer coefficients so calculated at about the time dissolved oxygen goes to zero agree fairly well with the values of the physical k_La obtained by other methods (Suresh et al., 1987a). However, in the period of increasing rates that sometimes followed the slow reaction regime, volumetric mass transfer coefficients increased much beyond this value. This suggests a modification of the concentration profile of oxygen close to the interface, as would happen if the reaction were to occur to a significant extent within the diffusion film.

Because of the small interfacial areas, the flat interface reactor represents a case of oxidation under small mass transfer rates. Oxidation experiments in the FIR showed the same general features as shown by the stirred-tank reactor, but there were important differences. The initial period of induction and slow reaction regime was very short lived; on the admission of the oxygen-nitrogen mixture into the reactor, the dissolved oxygen concentration started to increase, and then immediately

declined (without achieving saturation), quickly decreasing to zero. A prolonged diffusional regime followed, with the absorption rates remaining constant and the dissolved oxygen concentration remaining at zero. Mass transfer enhancements were never actually observed, even after prolonged reaction periods of 15–20 h at 433–436 K.

Development of product concentration with time

The results of chemical analysis for the experiment at 423 K in the STR are shown in Figure 2. The time at which dissolved oxygen goes to zero is shown in the figure. It is seen that the cyclohexane conversion data in the slow reaction regime follow a straight line on semilogarithmic coordinates. After dissolved oxygen goes to zero, however, a decrease in kinetic rates is seen.

The concentrations of cyclohexanol + hydroperoxide (OL + HP) and cyclohexanone (ONE) are also shown as a function of time in Figure 2. Except at small times (when the hydroperoxide levels are probably high), the concentration of ONE is higher than OL + HP. After an initial period in which the ketone concentrations follow a line of higher slope than total conversions of OL + HP, the slopes of all three lines are similar, as was found in the data from the batch microautoclaves. In experiments with an extended period of slow reaction, the lines were parallel over most of the duration of this regime.

The development of OL + HP, ONE, and adipic acid with time at 423 K is shown on arithmetic coordinates in Figure 3. Adipic acid is a secondary product of the oxidation and hence forms only at later stages of the oxidation. However, most of these samples were taken after the dissolved oxygen in the bulk liquid had disappeared and when mass transfer enhancements were being observed. The rapid buildup of adipic acid at later stages therefore could well be a consequence of mass transfer limitations. Both Figures 2 and 3 do show that when dissolved oxygen is absent in the liquid bulk, the concentration of the intermediates increases at smaller rates than before.

The development of the concentrations of OL + HP and ONE in the FIR is shown in Figure 4, and is representative of

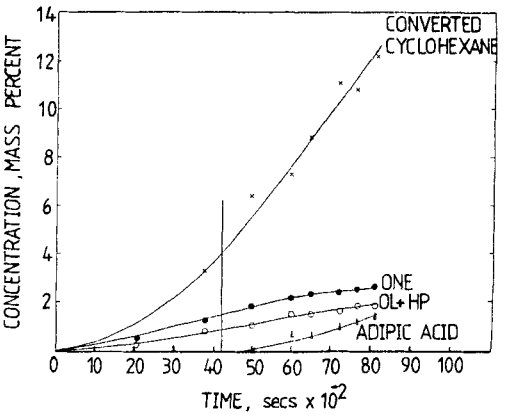

Figure 3. Build-up of intermediates and adipic acid at 423 K in stirred-tank reactor.

p_o = 0.33 bar; $U_G = 0.9 \times 10^{-2}$ m/s; RPS = 16.6

the kinetics in the diffusional regime. The stirrer speeds used are indicated. Although the mass transfer coefficient in the FIR is nearly proportional to the stirrer speed, the variation of the absorption rate is less than proportional to the variation in stirring speed, since a decrease in the absorption rate means an increase in the partial pressure of oxygen at the exit, (and vice versa), and this change in the driving force acts against the change in k_L. The concentrations of OL + HP are seen to be higher than those of ONE at all times by a factor of about 2, in striking contrast to the STR data discussed earlier. During the diffusional regime the reaction occurs in the bulk of the liquid, but takes place at negligible oxygen levels and hence under conditions of first-order kinetics in oxygen. The results show, therefore, that production and consumption of intermediates proceed by different routes under conditions of zero-order and first-order kinetics. Since product distributions in the STR are determined by the fairly long initial period in which the dissolved oxygen levels were high enough to ensure zero-order kinetics, the product distributions from the STR and the FIR cannot be compared. These results indicate that the different results seen in

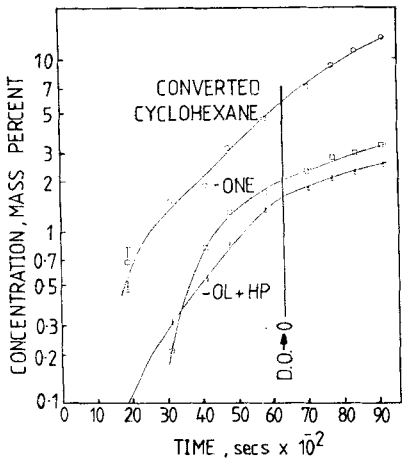

Figure 2. Conversion to total products and intermediates at 423 K run as Figure 1.

–ONE = cyclohexane; –OL = cyclohexanol; HP = hydroperoxide

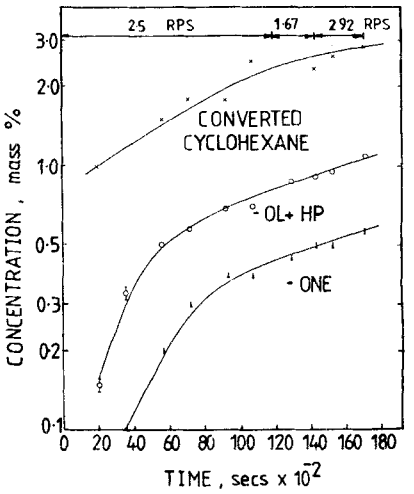

Figure 4. Build-up of total products and intermediates in flat interface reactor at 433 K.

the literature on the ratio of OL to ONE in the cyclohexane oxidate could well have resulted from different regimes of absorption being in operation.

Reproducibility of Absorption Rates and Dissolved Oxygen Levels in the STR

Figure 5 shows the variation of absorption rate and dissolved oxygen concentration with time in two experiments at 430 K conducted under almost identical conditions. The small differences can easily be explained by slight differences in the induction times, liquid level, and temperature through the experiments. Under the conditions of these experiments, oscillations in dissolved oxygen concentration at low concentrations were quite pronounced. The fact that oscillations occur at about the same time, conversion, and dissolved oxygen concentration in the two cases suggests that the oscillations are real and not some random fluctuations in the measurements.

The reproducibility of the results of chemical analysis in these two experiments is shown in Figure 6 and is seen to be satisfactory. The curves exhibit all the general features discussed in the previous section.

Mass Transfer with Chemical Reaction

The foregoing results indicate that in a typical experiment, there is a range of conversions where the dissolved oxygen concentration is zero, but the absorption rate keeps increasing. The rate of absorption is higher than the physical mass transfer rate at the same driving force and it is to be suspected that the concentration profile of oxygen in the vicinity of the gas-liquid interface is being modified by chemical reaction. Under such circumstances, diffusion and reaction can no longer be considered as processes occurring in series, but must be considered as occurring simultaneously. Film and penetration models have been traditionally used to analyze these situations, and in most cases lead to similar results (Astarita, 1967; Danckwerts, 1970). Mass transfer accompanied by an autocatalytic reaction of the first order (with respect to the dissolving gas) has been analyzed using both these models (Sim and Mann, 1975; Flores-Fernandez and Mann, 1978). It has been shown in these studies that enhancement factors in such cases can be much higher than in the case of nonautocatalytic reactions. In this paper, the film theory will be used to analyze the effect of chemical reaction on

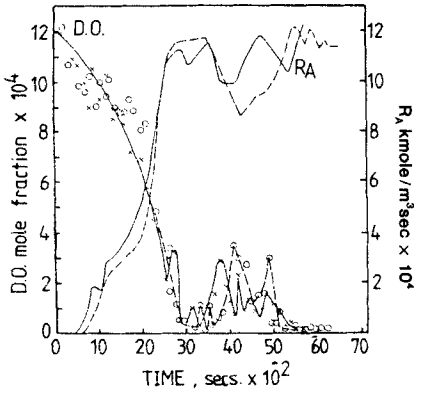

Figure 5. Reproducibility of stirred-tank reactor experiments.
Variation of dissolved oxygen concentration and absorption rate with time; temp. = 430 K

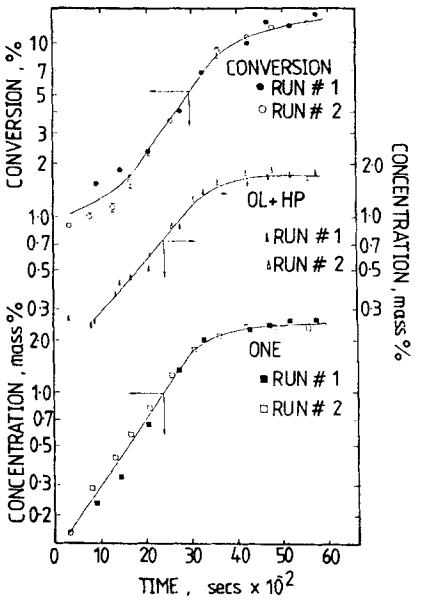

Figure 6. Reproducibility of stirred-tank reactor experiments.
Results of chemical analysis; temp. = 430 K

mass transfer in the oxidation of cyclohexane, using the kinetic model for the reaction developed elsewhere (Suresh et al., 1987b). The equations are solved for the cases of the reaction being partly or wholly in the diffusion film. Considerable simplification of the analysis and equations results when the concentration and the diffusivity of the products are sufficiently high for concentration profiles of products in the film to be neglected, leading to a pseudozero-order regime.

Theory of kinetically enhanced mass transfer coefficients

Although it has been shown that the kinetics become first order in oxygen at sufficiently small concentrations of oxygen, the concentration of oxygen close to the interface, and hence in most of the diffusion film, will be much higher than in the bulk. Therefore, the kinetics will be considered to be zero order in oxygen in the film theory equations.

The diffusion plus reaction equations in the film, in terms of the reaction scheme presented by Suresh et al. (1987b), can be written as:

Oxygen

$$D\frac{d^2c_o}{dx^2} = (k_{01}c_{Px} + k_{02}c_{Px}^2)H(c_o) \tag{1}$$

Reaction products

$$D_p\frac{d^2c_{Px}}{dx^2} = (-k_{01}c_{Px})\,H(c_o) \tag{2}$$

with the initial and boundary conditions

$$\text{at } x = 0,\ c_o = c^* \quad \text{and} \quad \frac{dc_{Px}}{dx} = 0 \tag{3}$$

$$\text{at } x = \delta,\ c_o = c_L \quad \text{and} \quad c_{Px} = c_p \tag{4}$$

These equations assume that the quasi-steady state assumptions, as regards free radical concentrations, made in deriving the kinetic expressions are satisfied at every point in the film. The function $H(c_o)$ on the righthand side of Eqs. 1 and 2 is the unit step function,

$$H(c_o) = 1 \text{ for } c_o > 0$$
$$= 0 \text{ otherwise}$$

and expresses the fact that the reaction cannot proceed in the absence of oxygen. Equation 3 states that equilibrium is achieved at the gas-liquid interface, and that the products do not transfer across the interface. The boundary condition, Eq. 4, has received some attention in the literature. An alternative boundary condition that is preferred by some authors (Darde et al., 1983; Haynes, 1983; and others) is an oxygen flux balance at the film-bulk interface:

$$-a D \left.\frac{dc_o}{dx}\right|_{x=\delta} = r_{\text{bulk}} \tag{5}$$

where r_{bulk} is the reaction rate of oxygen in the bulk. If Eq. 4 is used, the absorption rate is a function of c_L, and variation of c_L with time has to be obtained by way of a separate material balance on the liquid phase in the reactor. Equation 5 eliminates the need for this, and transition from one regime to the next comes about naturally as the reaction rates get faster and the dissolved gas concentration smaller. A pseudosteady-state assumption is implicit in both cases, since the initial and boundary conditions, which are in reality functions of time, have been regarded as constants in the film theory formulation.

Astarita (1967) has shown that for physically realistic values of the interfacial area and gas holdup, as long as the dissolved gas levels are not negligible the mass transfer is not chemically enhanced. The effect of the chemical reaction on the process of mass transfer is therefore only important at reaction rates higher than can cause the dissolved gas levels to go to zero. At such reaction rates, reaction begins to proceed to a significant extent within the diffusion film, and at high enough reaction rates the reaction is virtually complete within the film, no oxygen being able to escape into the bulk. This is the fast reaction regime.

Transition from slow to fast reaction regime

For this case, c_L in the boundary condition of Eq. 4 is zero. Since oxygen is available everywhere within the film, the step function on the righthand side of Eqs. 1 and 2 takes the value of unity and the equations can be solved easily. Equation 2 is first solved to get the variation of the concentration of products within the diffusion film. This result is then substituted in Eq. 1 and the equation solved to get the concentration profile of oxygen in the film. The profiles for the reaction products and oxygen in the film are:

$$\frac{c_{Px}}{c_p} = \frac{\cos\left[(x/\delta)\sqrt{(M_1/q)}\right]}{\cos\sqrt{(M_1/q)}} \tag{6}$$

$$\frac{c_o}{c^*} = 1 - (x/\delta) + \frac{q}{\cos\sqrt{(M_1/q)}}\left\{1 - \cos\frac{x}{\delta}\sqrt{(M_1/q)} - \frac{x}{\delta}\left[1 - \cos\sqrt{(M_1/q)}\right]\right\} + \frac{qM_2}{8M_1\cos^2\sqrt{(M_1/q)}} \cdot \left\{1 - \cos\left[\frac{2x}{\delta}\sqrt{(M_1/q)}\right] - \frac{x}{\delta}\left[1 - \cos 2\sqrt{(M_1/q)}\right]\right\} - \frac{M_2}{4\cos^2\sqrt{(M_1/q)}}\left\{(x/\delta)\left[1 - (x/\delta)\right]\right\} \tag{7}$$

where the dimensionless groups used are defined by

$$q = \frac{D_p c_p}{Dc^*}; \quad M_1 = \delta^2\frac{k_{01}c_p}{Dc^*} = \frac{Dk_{01}c_p}{k_L^2 c^*};$$
$$M_2 = \delta^2\frac{k_{02}c_p^2}{Dc^*} = \frac{Dk_{02}c_p^2}{k_L^2 c^*} \tag{8}$$

since $k_L = (D/\delta)$.

M_1 and M_2 compare the diffusion and reaction rates for the two oxygen-consuming reactions, namely, the reaction of oxygen with cyclohexane and the reaction of oxygen with the reaction products, respectively. The diffusion-reaction parameter $\sqrt{M}$ for the overall reaction of oxygen can be defined as:

$$\sqrt{M} = \frac{\sqrt{[2D\,(k_{01}c_p + k_{02}c_p^2)/c^*]}}{k_L} \tag{9}$$

From the concentration profile for oxygen, the absorption flux can be determined as,

$$N_A = -D\left.\frac{dc_o}{dx}\right|_{x=0} \tag{10}$$

and the enhancement factor, which is the ratio of the rate of mass transfer with chemical reaction to that without:

$$E = \frac{N_A}{(Dc^*/\delta)} \tag{11}$$

can be written:

$$E = 1 + \frac{q\left[1 - \cos\sqrt{(M_1/q)}\right]}{\cos\sqrt{(M_1/q)}} + \frac{qM_2\left\{1 - \cos\left[2\sqrt{(M_1/q)}\right]\right\}}{8M_1\cos^2\sqrt{(M_1/q)}} + \frac{M_2}{4\cos^2\sqrt{(M_1/q)}} \tag{12}$$

At higher and higher reaction rates, more and more of the oxygen absorbed is consumed by reaction within the film, and the flux of oxygen into the bulk decreases, finally reaching zero at the onset of the fast reaction regime. Since the flux of oxygen into the bulk is proportional to its concentration gradient at $x = \delta$, the condition at which the transition to the fast reaction regime is complete can be written as:

$$\left.\frac{dc_o}{dx}\right|_{x=\delta} = 0 \tag{13}$$

which gives

$$\frac{q}{\cos\sqrt{(M_1/q)}}\left[\sqrt{(M_1/q)}\sin\sqrt{(M_1/q)} - 1 + \cos\sqrt{(M_1/q)}\right] + \frac{qM_2}{8M_1\cos^2\sqrt{(M_1/q)}}\{2\sqrt{(M_1/q)}\sin[2\sqrt{(M_1/q)}] - 1 + \cos[2\sqrt{(M_1/q)}]\} + \frac{M_2}{4\cos^2\sqrt{(M_1/q)}} = 1 \quad (14)$$

Fast reaction regime

If the reaction rate is higher than what is required to satisfy Eq. 14, the oxygen is totally consumed within the film. In general, in the fast reaction regime only a part of the film, $0 \leqq x \leqq \lambda$, contains oxygen and no oxygen can diffuse into the liquid beyond $x = \lambda$. The step function in the concentration of oxygen on the righthand side of Eqs. 1 and 2 means that in this case the diffusion-reaction equations for oxygen and cyclohexane have to be solved only in the region $0 \leqq x \leqq \lambda$ and we have the following at $x = \lambda$:

$$c_o = 0 \quad \text{and} \quad \frac{dc_o}{dx} = 0 \quad (15)$$

and

$$c_p = c_{p_\lambda}$$

In the rest of the film, that is, in the region $\lambda \leqq x \leqq \delta$, while the oxygen concentration is zero, the concentration of the products satisfies the pure diffusion equation. The depth of penetration of the gas, λ, can be determined from the condition that the concentration gradient at this distance from the interface is zero. This condition gives λ as the solution to the equation

$$\frac{M_2 z^2}{4\cos^2\theta}(c_{p_\lambda}/c_p)^2\{1 + (1/\theta)[\sin 2\theta + (\cos 2\theta - 1)/(2\theta)]\} + \frac{M_1 z^2}{\theta\cos\theta}(c_{p_\lambda}/c_p)\,[\sin\theta + (\cos\theta - 1)/\theta] = 1$$

where

$$z = (\lambda/\delta) \quad \text{and} \quad \theta = z\sqrt{(M_1/q)} \quad (16)$$

The concentration c_{p_λ} at $x = \lambda$ can be determined by equating the diffusive flux of the products from the region of $x \leqq \lambda$:

$$\frac{c_{p_\lambda}}{c_p} = \frac{1}{1 + (z-1)\sqrt{(M_1/q)}\tan\theta} \quad (17)$$

The concentration profiles of the reaction products and oxygen are given by,

Region $0 \leqq x \leqq \lambda$

$$\frac{c_{px}}{c_{p_\lambda}} = \frac{\cos[(x/\delta)\sqrt{(M_1/q)}]}{\cos\theta} \quad (18)$$

$$c_o/c^* = 1 - \frac{x}{z\delta} - \frac{q(c_{p_\lambda}/c_p)}{\cos\theta}\left\{\cos[(x/\delta)\sqrt{(M_1/q)}] - 1 - \frac{x}{z\delta}(\cos\theta - 1)\right\} - \frac{qM_2(c_{p_\lambda}/c_p)^2}{8M_1\cos^2\theta}\cdot\left\{\cos[(2x/\delta)\sqrt{(M_1/q)}] - 1 - \frac{x}{z\delta}(\cos 2\theta - 1)\right\} - \frac{zM_2}{4\cos^2\theta}(c_{p_\lambda}/c_p)^2(x/\delta)\left(1 - \frac{x}{z\delta}\right) \quad (19)$$

Region $\lambda \leqq x \leqq \delta$

$$\frac{c_{px}}{c_p} = (x/\delta)\frac{(c_{p_\lambda}/c_p) - 1}{z - 1} + \frac{z - (c_{p_\lambda}/c_p)}{z - 1} \quad (20)$$

$$c_o = 0 \quad (21)$$

The enhancement factor is given by

$$E = (1/z) + \frac{(zM_2/4)(c_{p_\lambda}/c_p)^2}{\cos^2\theta} - (q/z)(c_{p_\lambda}/c_p)\frac{\cos\theta - 1}{\cos\theta} - (c_{p_\lambda}/c_p)^2\frac{qM_2(\cos 2\theta - 1)}{8M_1 z\cos^2\theta} \quad (22)$$

Enhancement factors

The enhancement factor, as can be seen from Eqs. 12 and 22, is in general a function of the diffusion-reaction parameter $\sqrt{M}$, the group q, and the ratio of the rates of the two oxygen-consuming reactions, M_2/M_1. Computed values in the transition from slow to fast reaction and in the fast reaction regime are shown in Figure 7. The point of onset of the fast reaction regime is indicated on the curves; at enhancements higher than 2–3, the reaction is seen to be complete within the diffusion film. The higher the value of $\sqrt{M}$, the higher is the effect of chemical reaction on mass transfer.

At a given value of $\sqrt{M}$, the enhancement factors are higher for smaller values of q and M_2/M_1. The parameter q is a measure of the ability of the reaction products to diffuse away from the site of the reaction and keep the concentration gradients

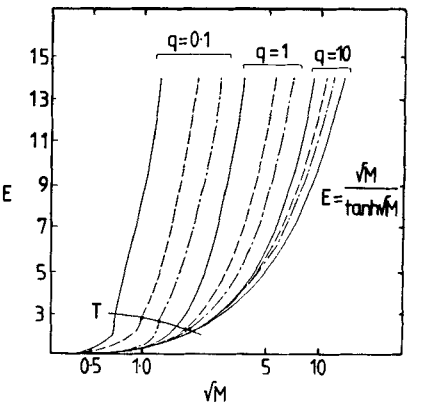

Figure 7. Enhancement factors vs. *M*.
Values of M_2/M_1 are: —, 0; ---, 2; ····, 5. Curve T shows the completion of the transition to fast reaction.

small within the film. The smaller the value of q, the steeper are the concentration gradients within the film, and the higher concentration of the products within the film leads to higher enhancement of the mass transfer because of the dependence of oxygen consumption rate on product concentration. The effect of the ratio of the rates of the secondary and primary processes of oxygen consumption, M_2/M_1, can be interpreted as follows. A low value of this ratio means that the primary reaction is much faster than the secondary reactions, and since this is the reaction that produces the autocatalytic products, a higher rate of this reaction leads to higher enhancements. In the proposed mechanism, the secondary reactions only convert the autocatalytic products from one form to another and do not lead to a net increase in their concentration.

Pseudozero-order reaction in the film

At very high values of q and/or M_2/M_1, the curves collapse into a common asymptote. This represents the case of mass transfer with pseudozero-order reaction. The approximate solution given by Hikita and Asai (1964) for a pseudo mth-order reaction, namely

$$E = \frac{\sqrt{M}}{\tanh \sqrt{M}} \tag{23}$$

agrees very well with the present solutions under these conditions.

In a general problem of mass transfer with a (m, n)th order reaction (mth order in the gas and nth order in the liquid phase reactant), the pseudo mth-order case arises when the diffusion of the liquid phase reactant is fast enough to keep its concentration gradient within the diffusion film down to negligible values. In normal (i.e., nonautocatalytic) reactions this asymptote represents the maximum enhancement achievable at a given value of $\sqrt{M}$. By contrast, in the present case, it is seen to represent the minimum enhancement possible at a given $\sqrt{M}$. This difference is behavior between normal reactions and autocatalytic reactions can be explained as follows. In normal reactions, if the liquid phase reactant is unable to diffuse fast enough to maintain a uniform concentration within the film, the concentration of this reactant is less within the film than it is within the bulk, and hence the reaction rate is less than it would be if the bulk concentration were to prevail. In the present case, however, such an inability of the diffusion of the liquid phase species (which is the totality of reaction products) to keep pace with the reaction results in an accumulation of this species in the film, leading to reaction rates higher than in the pseudozero-order case. Products are produced at higher rates in the film, and this leads to more severe diffusion limitations. This snowballing effect explains the steep increase in the enhancement factor with $\sqrt{M}$ at small values of q. These results therefore confirm that autocatalysis can lead to mass transfer limitations that are more severe than would be expected in normal reactions.

Equations for the case of pseudozero-order reaction, much simpler in form than the equations derived earlier, can be derived from the latter by making the approximation $\sqrt{(M_1/q)} = 0$. The transition to the fast reaction regime is complete under these circumstances when

$$\sqrt{M} = 2 \tag{24}$$

and the enhancement factors are given, during the transition from slow to fast reaction, by

$$E = 1 + M/4 \tag{25}$$

and in the fast reaction regime by

$$E = \sqrt{M} \tag{26}$$

Comparison with Experimental Data

In Figure 8 the experimentally observed enhancement factors have been plotted as a function of the parameter $\sqrt{M}$. The data were obtained in the two gas-liquid contactors from the absorption rates after the dissolved oxygen from the liquid bulk was reduced to zero. The data cover several temperatures and diverse mass transfer conditions (as determined by the partial pressures of oxygen used, stirrer speed, etc.). Because of the low solubility of oxygen in cyclohexane at the conversions at which these enhancements were observed, the values of q are quite high, even after accounting for the possible differences in diffusivities between the reaction products and oxygen. (The correlation for diffusion coefficients given by Sridhar and Potter [1977] indicates that the diffusivity of cyclohexanone is about 2.5 times lower than that of oxygen in cyclohexane; with this ratio, the lowest value of q obtained was about 40, with most of the values being well over 100). The value of the group M_2/M_1 was higher than 3–4 for these data. A reference to Figure 7 shows that the reaction can be considered to be pseudozero-order under these conditions. The enhancement factors have been calculated, assuming the gas phase to be well mixed, by dividing the measured absorption rates by the saturation concentration of oxygen at the outlet partial pressure and the known (physical) volumetric mass transfer coefficient. In the calculation of the factor $\sqrt{M}$, the mass transfer coefficients and solubilities of oxygen in pure cyclohexane have been used. Solubility

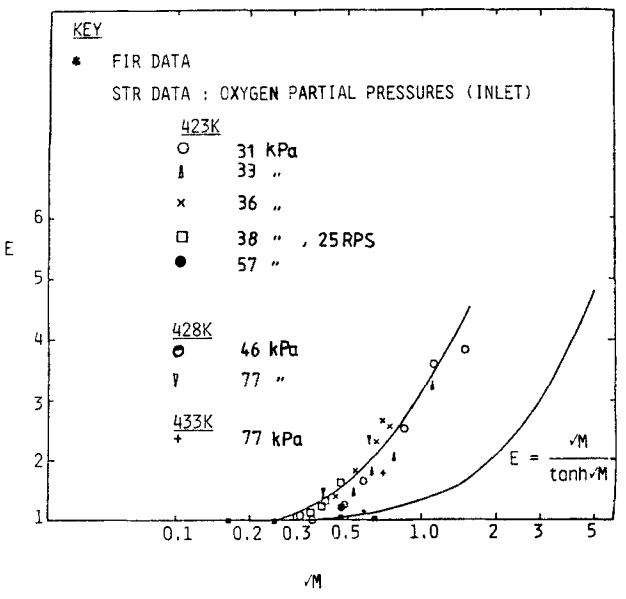

Figure 8. Enhancement factors: theory and experiment.
Stirrer speed 16.6 RPS unless otherwise indicated

measurements have indicated a negligible effect of conversion. Determination of the volumetric mass transfer coefficient in reacted liquid (conversion = 11–12%) from the measured absorption rates and concentration driving force at 413 K yields a value only 15% lower than the value expected in pure cyclohexane. The rate constants used are taken from Suresh et al. (1987b).

Consideration has been restricted to conversions of less than about 12%, except in the case of the FIR, where the conversions were artificially boosted by dosing with products to about 15% to achieve $\sqrt{M}$ values of 0.73 (this was necessary because of the higher mass transfer coefficients in the FIR). The data at higher conversions gave enhancements that were lower than the experimental curve shown.

It is noted that the STR data from a variety of conditions are satisfactorily brought together in the plot. The scatter is no more than is to be expected. However, the experimental data show enhancements much higher than predicted by the film theory, as seen by a comparison of the experimental curve with the pseudozero-order asymptote plotted for comparison. The theoretical curve is displaced from the experimental to the right by a factor of 3 over the entire range of enhancements observed. Since the kinetics have been shown to describe the experimental data in the slow reaction regime quite satisfactorily and since the kinetic rates affect the enhancements only to the extent of their square root under the conditions of pseudozero-order reaction, the reason for this discrepancy is unlikely to lie in the kinetics.

A plot of E vs. $\sqrt{M}$ has rarely been published in the literature for a sparged and stirred reactor. The twin uncertainties of the hydrodynamics on the one hand and the interfacial area on the other make a test of the theories of mass transfer with chemical reaction very difficult in the bubbling stirred-tank reactor. The usual approach is to assume the theory to be valid and estimate the interfacial area from the absorption rates in the fast reaction regime. This constitutes the chemical method for the determination of interfacial area. In the present work, the E–$\sqrt{M}$ plot has been constructed using the interfacial areas that follow from the physical measurements of Sridhar and Potter (1980b). If the interfacial area were to be estimated using the chemical method from the present data, the extent of the discrepancy in Figure 7 indicates that the calculated areas will be about three times the estimated physical areas. It is interesting to note that the interfacial areas measured by the chemical method are generally higher than the physically measured areas, and the extent of the discrepancy is about a factor of 2–3 (Sridhar and Potter, 1978). Looked at this way, Figure 8 indicates a problem that has generally been experienced in the application of the theories of mass transfer to the bubbling stirred tank.

Based on the above arguments, some differences might be expected to emerge between the data from the sparged reactor and the flat interface reactor. The data from the FIR, also shown in Figure 8, show no enhancement in mass transfer up to values of $\sqrt{M}$ of about 0.73, as predicted by the theoretical curve. Although it would be more conclusive to show genuine enhancements such as are predicted by theory at large values of $\sqrt{M}$, the conversions necessary to go to values of $\sqrt{M}$ of 2 or above (at which values the existence of the fast reaction regime can be verified by showing an independence of the absorption rates with respect to stirrer speed) are well above the conversion range in which the kinetic model can be confidently used.

The complexity of the hydrodynamics in an STR, which results in fairly strong local variations in most parameters that determine the absorption rate, has been recognized. It may be argued that the hydrodynamics do not matter in the fast reaction regime, since the reaction is completed so close to the interface that the hydrodynamic parameter (for example, the film thickness in the film theory) is of no importance (Astarita, 1967). While this may be true at large enhancements (when the reaction is sufficiently fast in all parts of the reactor to proceed in the fast reaction regime despite local variations in mass transfer coefficients, interfacial areas, etc.), at small enhancements such as have been observed in the present experiments it is possible for different regimes to exist in different parts of the contactor. The overall absorption process under these conditions can show a dependency on the hydrodynamics. Sridhar and Potter (1978) attribute the differences they found in the interfacial areas as measured by the physical and chemical methods to such local variations.

In order to investigate the effects of a plug flow of gas, the oxidation in the STR was simulated over the entire period of an experiment, including that of enhancement. Plug flow of gas was assumed, and the expressions for the absorption rate in the various regimes for the case of pseudozero order were used. As expected, the predictions did not differ much in the slow reaction regime. At the high levels of depletion toward the end of the slow reaction regime and beyond, the plug flow assumption predicted higher rates but did not predict an increase in the rates in the manner seen in the experiment, the predicted rates again leveling off once dissolved oxygen reached zero.

It might be recalled that even in the mass transfer studies (Suresh et al., 1987a), the behavior of the bubbling reactor could not be readily accounted for by theory, while the FIR behaved quite according to expectations. One of the explanations offered was that interactions between bubbles could lead to an apparent lowering of mass transfer rates in physical absorption. If such interactions exist, their effect would diminish as the effect of the reaction close to the interface begins to steepen concentration profiles, and an increase in the mass transfer rates would be observed. It will be appreciated that the concentration profiles of oxygen close to the interface would need to be modified by reaction before such an effect would be observed. A bubble-based model of the STR that takes into account some forms of interaction and a residence time distribution (RTD) in the gas phase different from that of a well-mixed vessel are obviously needed.

Mass transfer with chemical reaction from bubble swarms in a stirred tank

Theories of interphase mass transfer are usually concerned with local phenomena at any position in the gas-liquid contactor, and a rigorous prediction of global transfer rates from these theories, in the face of strong local variations that exist in a contactor of such complexity as the bubbling STR, requires a detailed knowledge of the flow paths of the gas and liquid within the vessel. The magnitude of the problem is enormous. Carpenter (1986) discusses the work that has been aimed at a detailed understanding of the hydrodynamics in the STR. Even approximate analyses of this nature require the use of a digital computer, and the commonly used numerical schemes often run into difficulties in such computations. A less ambitious approach would be to develop simplified models for the transfer process

from the bubbles, and attempt to address the questions of gas phase mixing and interaction between bubbles in at least an approximate manner.

A model is presented in this paper which assumes a residence time distribution for the gas bubbles that is in approximate agreement with experimental data. Expressions for the case of mass transfer with a first-order chemical reaction are developed, which can easily be simplified to treat physical mass transfer. An approximate treatment of the case of zero-order reaction in the liquid is presented and compared with the experimental data on the oxidation of cyclohexane.

Gal-Or and Resnick (1964) pioneered a bubble-based treatment of the STR. By using the (physically measurable) residence time in the gas phase in place of the (largely conceptual) surface life of liquid elements in the traditional penetration-type approaches, their work enables transfer rates in the contactor to be calculated directly from first principles. The bubbles were assumed not to mix during the course of their journey through the contactor. These authors assumed all bubbles to have the same residence time in the contactor and to transfer the solute by a process of unsteady state transfer to the surrounding liquid, which stayed with the bubbles throughout their journey through the contactor.

The two assumptions, namely that the bubbles do not intermix in their entire journey through the contactor and that the liquid element to which a bubble transfers its solute is not replaced during this period, should be regarded as unrealistic, the latter in spite of the fact that the experimental mass transfer coefficients in the system oxygen-cyclohexane in this work do indicate a reduction in surface renewal frequencies at high temperatures.

The model to be discussed is similar in approach to that of Gal-Or and Resnick (1964), but some of the assumptions are modified to better accord with experimental observations. The gas bubbles are assumed to be spherical and all of the same size. Gal-Or and Hoelscher (1966) have investigated the effect of imposing a bubble-size distribution on models of the type proposed by Gal-Or and Resnick (1964) and show that little error results by replacing the variable bubble radius by the Sauter mean bubble radius. The gas-liquid interfacial area and the gas holdup are assumed to be uniform everywhere within the vessel at their vessel-average values.

The first assumption different from those of Gal-Or et al. (1964) is that the stirrer contactor is assumed to be made up of two zones in series. The liquid concentration is the same in both the zones, in accordance with the experimental evidence that suggests the liquid to be well mixed under most circumstances. The second assumption that differs from those of Gal-Or et al. is that the ages of the gas bubbles in each zone are distributed as in a perfectly well mixed vessel. Further, the gas from the bubbles leaving the first zone is completely mixed in the impeller zone and redispersed as fresh bubbles at the well-mixed concentration. This mixing-redispersion process is assumed to be instantaneous. Thus the gas that enters the contactor as bubbles initially circulates in the first zone, then is recycled to the impeller zone where the contents of the bubbles are mixed and redistributed, the new bubbles circulating in the second zone before leaving the vessel. The existence of two mixing zones in a sparged and stirred vessel, one above the impeller and one below, has been commented on by several workers (Hanhart et al., 1963; Mann, 1986), and indeed can be observed when the liquid circulation caused by the agitator is strong enough to disperse the gas throughout the vessel (Mann, 1986). The studies of Hanhart et al. showed a residence time distribution in the gas phase intermediate between what is expected of a single well-mixed vessel and two well-mixed vessels in series, and the studies of Gal-Or and Resnick (1966) showed it to be similar to the RTD of two well-mixed vessels in series with a small fraction of the gas moving in plug flow.

The mean residence time of the gas in each of the two well-mixed zones is assumed to be the same, although the treatment is easily extended to different residence times in the two zones. Within each zone, the bubbles are assumed to retain their identity. Each bubble, on its formation, picks up a spherical shell of liquid that remains with it throughout its life in the zone and transfers solute to it by unsteady state diffusion. A first-order reaction is assumed to be taking place in the liquid. The volume of liquid available to each bubble is determined by the relative volume of gas and liquid in the contactor. In other words, the dispersion is looked upon as being made up of a number of spherical model cells, each with a gas bubble at its center. Each model cell is supposed to behave as a rigid body, and convective diffusion effects are neglected.

The concentration profiles in the liquid surrounding a bubble in a swarm must, in general, be considered to be influenced by the presence of neighboring bubbles. This interaction is taken into account in the present model by the finite volume of liquid available to each bubble, and also by postulating that the diffusive flux of the solute midway between two bubbles (i.e., at the outer radius of the model cell) is zero.

Equilibrium is assumed to prevail at the interface and the mass transfer resistance in the gas phase is assumed to be negligible. Due to absorption, the partial pressure of the solute in a gas bubble varies as it moves through the liquid, and there is a consequent variation of the interfacial concentration in the liquid. The gas is assumed to be lean in the solute so that the change in the size of the bubble due to absorption can be neglected. Considering the first zone, the variation of the interfacial concentration c^* as a function of the age of the bubble, τ, can be found by a material balance for the solute in the gas bubbles. Equating the decrease in the amount of solute in a bubble in a differential time $d\tau$ to the amount tranferred into the liquid, we get

$$\frac{dc^*}{d\tau} = K^* \left.\frac{\partial c_o}{\partial r}\right|_{r=r_b} \tag{27}$$

where

$$K^* = \left(\frac{3H'_o RTD}{r_b}\right) \tag{28}$$

The equations and the initial and boundary conditions for diffusion and chemical reaction in spherical coordinates for the model cell (because of symmetry only the radial variation of the concentration needs to be considered) can now be written as

$$\frac{D}{r^2}\frac{\partial}{\partial r}\left(r^2 \frac{\partial c_o}{\partial r}\right) = \frac{\partial c_o}{\partial \tau} + kc_o \tag{29}$$

at $\tau = 0$, $r_b \leq r \leq b$, $c_o = c_L$

and at $r = r_b$, $c_o = c^* = c_i^*$ (30)

at $r = r_b$, $\tau > 0$, $c_o = c^*$ and $\dfrac{dc^*}{d\tau} = K^* \dfrac{\partial c_o}{\partial r}\bigg|_{r=r_b}$ (31)

at $r = b$, $\tau > 0$, $\dfrac{\partial c_o}{\partial r} = 0$ (32)

where b is the outer radius of the model cell, r_b is the bubble radius, r is the radial distance from the center of the bubble, and k is the first-order reaction rate constant. c_L is the concentration of the liquid into which the bubble is released and c_i^* is the interfacial concentration at the instant the bubble is formed. c_L is assumed to be time-invariant in the time scale of bubble lifetime; in a batch reactor of the type used in the present studies, this amounts to assuming a pseudosteady state in the liquid phase. With the substitution

$$Z = c_o r \tag{33}$$

the equation and the initial and boundary conditions take the form,

$$D \frac{\partial^2 Z}{\partial r^2} = kZ + \frac{\partial Z}{\partial \tau} \tag{34}$$

with

$$\begin{aligned} &\tau = 0, \quad r_b \leq r \leq b, \quad Z = c_L r \\ &r = r_b, \quad Z = Z_o^* = c_i^* r_b \\ &r = r_b, \quad \tau > 0, \quad Z = Z^* = c_o^* r_b \end{aligned} \tag{35}$$

$$\frac{dZ^*}{d\tau} = K^* \left(\frac{\partial Z}{\partial r}\bigg|_{r=r_b} - \frac{Z^*}{r_b} \right) \tag{36}$$

$$r = b, \quad \tau > 0, \quad \frac{\partial Z}{\partial r}\bigg|_{r=b} = \frac{Z_L}{b} \tag{37}$$

where

$$Z_L = b c_o(b)$$

The instantaneous absorption flux from a bubble of age τ is given by

$$N_A = -D \frac{dc_o}{dr}\bigg|_{r=r_b} = -\frac{D}{r_b} \frac{\partial Z}{\partial r}\bigg|_{r=r_b} + \frac{DZ^*}{r_b^2} \tag{38}$$

Since at any time, the zone contains bubbles of all ages, the average absorption flux in the zone can be calculated using the distribution of bubble ages in the zone, as

$$N_{A1} = \int_o^\infty N_A f(\tau) d\tau \tag{39}$$

Since the bubble ages in the zone are distributed as in a perfectly mixed vessel, the distribution of internal bubble ages is given by,

$$f(\tau) d\tau = (1/\tau) \exp(-t/\tau) d\tau \tag{40}$$

Since, at any time, the zone contains bubbles of all ages, the average where τ is the mean residence time in the zone. With this definition, it is seen that the average absorption flux is simply related to the Laplace transform of the instantaneous absorption flux, the Laplace parameter p being identified with the reciprocal of the mean residence time.

The instantaneous absorption flux can be calculated, using Eq. 38, as,

$$N_{A1} = \frac{D_P}{K^*} \left[\frac{1}{1 + (pr_b/K^*)\psi_2(\phi)} \right] \left[c_i^* - \frac{c_L}{p + k} \right] \tag{41}$$

where

$$p = 1/J$$

and

$$\psi_2(\phi) = \frac{1}{[1 + r_b \phi \psi_1(\phi)]} \tag{42}$$

$$\psi_1(\phi) = \frac{(b\phi - 1)\exp(-2r_b\phi) - (b\phi + 1)\exp(-2b\phi)}{(b\phi - 1)\exp(-2r_b\phi) + (b\phi + 1)\exp(-2b\phi)} \tag{43}$$

and

$$\phi = \sqrt{[(p + k)/D]} \tag{44}$$

The partial pressure of the solute in the gas phase at the exit of the zone is related to the interfacial concentration at equilibrium with it. The latter can be found by averaging the interfacial concentrations in all the bubbles at the exit of the zone. Since the distribution of exit ages in the well-mixed zone is again given by Eq. 40, the average interfacial concentration at the exit of the zone is given by

$$c_1^* = \frac{c_L p}{k + p} + \left(c_i^* - c_L \frac{p}{k + p} \right) \cdot \frac{(pr_b/K^*)}{1 + (pr_b/K^*) + r_b \phi \psi_1(\phi)} \tag{45}$$

The average absorption flux in zone 2 can be calculated in the same manner as before, except that c_1^* takes the place of c_i^*. This is because the zones are identical except for the fact that the partial pressure of the solute in the bubbles at the start of zone 2 is the average partial pressure of the gas at the exit of zone 1.

It should be noted that the calculation of the absorption rate in the model requires the use of no fitted parameters. All the model parameters are, or can be related to, known or measurable quantities in the contactor. Thus the outer radius of the model b is related to the bubble radius r_b and the gas holdup as $(r_b/b)^3 = H_G$.

The absorption rate in the reactor per unit volume of the dispersion can be calculated from the absorption flux by multiplying by the interfacial area per unit volume, which is again related to the bubble radius and the gas holdup as

$$a = 3H_G/r_b \tag{47}$$

Zero-order Reaction

The oxidation of cyclohexane can be regarded as a zero-order reaction in the region close to the gas-liquid interface, even when the concentration of dissolved oxygen in the liquid bulk is quite small. Since the model is to be evaluated on the basis of its predictions of the absorption rate in the oxidation of cyclohexane, the case of a zero-order reaction is of immediate interest. Unfortunately, the equations become complicated and difficult to solve in this case. An approximate analysis, on the lines suggested by Hikita and Asai (1964), is still possible, however. Comparing the definition of the diffusion-reaction parameter M used in the film theory analysis for a first-order reaction with that for a zero-order reaction, we can define an equivalent first-order reaction rate constant for a zero-order reaction as

$$k'_{ps} = 2r/c^* \tag{48}$$

where r is the reaction rate possible at the bulk concentration of the liquid phase reactant and the interfacial concentration of the gas. The zero-order reaction can now be treated as if it were a first-order reaction with the rate constant defined in Eq. 48. In the present case, however, even with this approximation Eq. 39 is difficult to solve, since it involves c^* in the reaction rate term, which is a function of bubble gas as given by Eq. 37. Therefore, as a further simplification, c^* in Eq. 48 is replaced by the average value at the exit of the zone, as given by Eq. 45, to define an equivalent first-order rate constant for the zone

$$k_{ps} = 2r/c_z^* \tag{49}$$

where c_z^* stands for the value of c^* at the exit of the zone. For the rate of reaction r, the zero-order rate expressions derived previously (Suresh et al., 1987b) can be used.

Comparison of Theory with Experiment

In Figures 9–12 the absorption rates measured during typical oxidation experiments in the temperature range 413–433 K under different mass transfer conditions are compared with the rates predicted by the model. The model has been used to predict both the physical and the chemical absorption rates. The rates for physical absorption are easily predicted from the equations

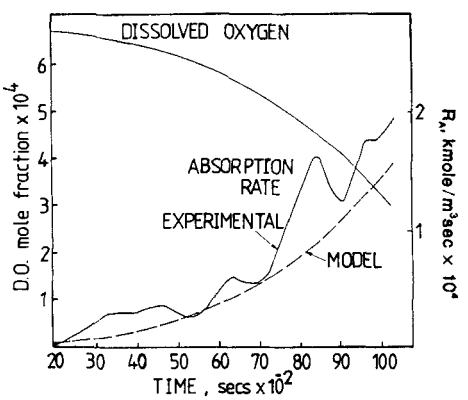

Figure 9. Model predictions and experimental results at 413 K.

p_o = 0.43 bar; $r_b = 0.965 \times 10^{-3}$ m; H_G = 11%
Mean residence time of gas in reactor = 1.82 s

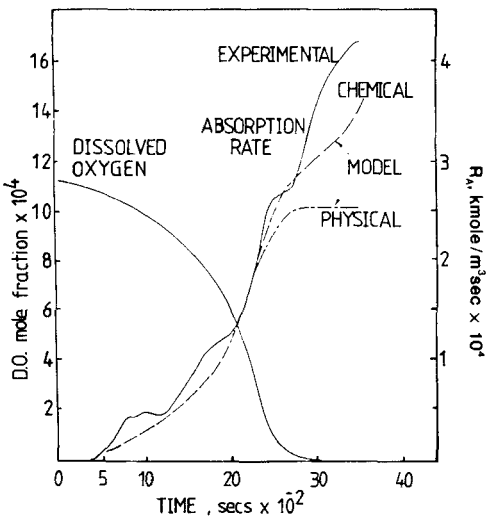

Figure 10. Model predictions and experimental results at 423 K.

p_o = 0.36 bar; $r_b = 0.91 \times 10^{-2}$ m; H_G = 13%
Mean residence time of gas in reactor = 2 s

derived for chemical absorption by using a rate constant of zero. In the calculation of chemical absorption rates, since the rate constant applicable to each zone is dependent on the concentration of the gas that leaves the zone, an iterative procedure is required. Using a trial value (which can be the concentration of the gas at the inlet), successive approximations can be calculated using Eq. 45 and the convergence is rapid. The predictions have been performed using the experimentally determined dissolved oxygen and product concentrations (the curve drawn through the experimental dissolved oxygen concentrations, which was used in these calculations, is also shown in the figures). The bubble diameter and gas holdup required for the calculations using the model have been estimated using the correlations of Sridhar and Potter (1980a).

In the region where free oxygen is available in the liquid, the absorption rates predicted by the model agree very well with the experimental absorption rates. The agreement is particularly

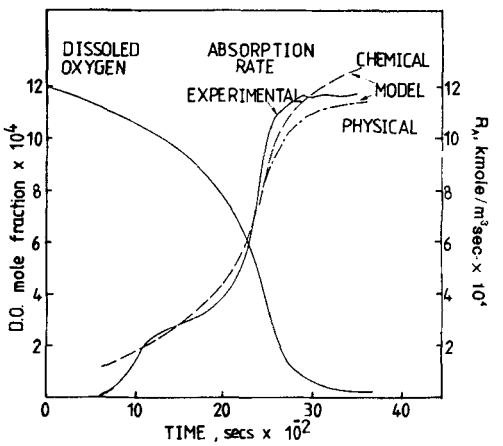

Figure 11. Model predictions and experimental results at 430 K.

p_o = 0.87 bar; $r_b = 1.01 \times 10^{-3}$ m; H_G = 21.6%
Mean residence time of gas in reactor = 1.54 s

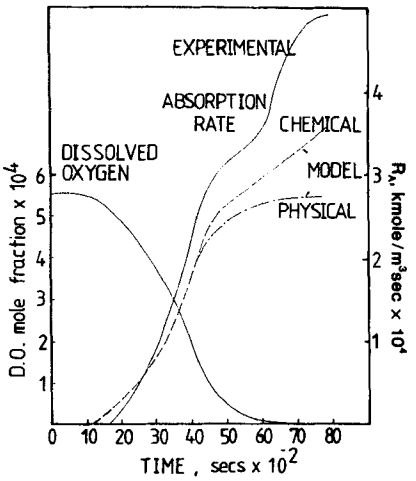

Figure 12. Model predictions and experimental results at 433 K.

p_o = 0.77 bar; r_b = 1 × 10^{-3} m; H_G = 21%
Mean residence time of gas in reactor = 1.51 s

good in Figures 11 and 12, which are cases of high gas holdup and hence, possibly of higher interaction between bubbles than the others. When dissolved oxygen levels are high, the model predicts reaction to have very little effect on the absorption rates, as seen by the fact that the chemical and physical absorption rates practically coincide in this case. Since dissolved oxygen concentrations from the experiment are being used in the model calculations, and since the model has no fitted parameters, the predictions performed are equivalent to predicting the average volumetric mass transfer coefficient for the entire reactor from first principles. It is seen that the model is able to perform this function well.

When the reaction becomes fast enough to keep the dissolved oxygen in the liquid bulk at negligible levels, it begins to have an effect on mass transfer rates, as seen by the increase in the separation between the physical and chemical curves in Figures 10–12. Two of the cases considered, Figure 10 and Figure 12, were experiments that produced enhanced mass transfer coefficients after the dissolved oxygen concentration had decreased to zero. In these cases the discrepancy between theoretical and experimental absorption rates is seen to increase in the region where no free oxygen is available in the liquid. However, because of the effect of chemical reaction, the present theory predicts that the absorption rate will continue to increase in this region, while the film theory does not. Equivalent predictions in this region can be made with the film theory (which, however, has to use the experimentally measured mass transfer coefficients) using the equation,

$$\text{kmol oxygen absorbed/s} = q_i - c_o^*(G_2/P_R H_o \rho_m) = Ek_L a c_o^* V_{GL} \qquad (50)$$

which assumes the gas phase to be well mixed. The film theory under these conditions predicts E to be 1, and hence Eq. 50 predicts a constant c_o^* and absorption rate at all times after dissolved oxygen goes to zero in Figures 11 and 12.

The superiority of the predictions of the present model to those of the film theory in this instance is probably a combined result of the low surface renewal frequencies assumed and the effects of interaction between bubbles, which have been accounted for by the boundary condition Eq. 37 and the finite volume of liquid available to each bubble. The approximate calculations performed showed that the effects of interaction between bubbles cannot be neglected at the experimentally observed holdups, at the penetration depths possible, because of the low surface renewal rates and high diffusivities. A contributing factor to the increase in the discrepancy between theory and experiment in the region of negligible dissolved oxygen could be the formation of the frothy layer in the experiment at these conversions, which makes bubble diameters and gas holdup more uncertain in this region; the phenomena responsible for the froth could also have an indirect effect on the residence time distribution of the gas bubbles.

Conclusions

The oxidation of cyclohexane, with its kinetic features, has been analyzed in the framework of the film theory of mass transfer with chemical reaction. The theoretical computations show that in such cases of autocatalytic, consecutive reactions, the enhancement factors can be much larger than in the case of non-autocatalytic reactions. The ease with which the products can diffuse away from the site of the reaction and the relative rates of the primary and secondary reactions have a profound influence on the enhancement factors. One would expect the same factors to influence the selectivity to the intermediates as well. Since the diffusion-reaction parameter varies inversely as the partial pressure of oxygen, and since the partial pressures of oxygen in industrial reactors are maintained low in the interest of safety, the existence of mass transfer limitations, and hence the possibility of the selectivities being adversely affected, should be seriously considered in the industrial context.

While the concentrations of oxygen and of the products in the present case suggest that the concentration profile of the products within the film can be considered flat, the experimentally observed enhancements in the sparged and stirred reactor are much higher than those predicted by the film theory for such conditions. Closer inspection suggests that such discrepancies are a result of the complexity of the contactor rather than of the reaction. The discrepancies observed between physically measured and chemically determined interfacial areas in literature studies on such contactors, and the agreement between theory and experiment observed in this work in the case of the flat interface reactor, lend some substance to this viewpoint. It may be recalled that the two types of gas-liquid contactors used exhibited substantial differences even in the physical mass transfer studies.

It is generally agreed that the various theories of mass transfer predict the effect of chemical reaction on mass transfer to be similar, in spite of differences in the physical picture on which they are based, provided a consistent definition of the mass transfer coefficient is used to treat the cases of physical and chemical mass transfer. This is often assumed to hold true even in mass transfer from bubble swarms, where effects of interaction between bubbles might be important. However, it is seen from the results of the present work that while the film theory is unable to account for the observed increase in mass transfer rates due to chemical reaction, a theory that accounts for the effects of interactions on mass transfer from bubbles in an approximate manner is able to predict, at least qualitatively, this increase. The theory is also able to predict quantitatively the

physical mass transfer coefficient from first principles, a fact that lends some support to the grounds on which the model is based. While still probably a grossly oversimplified picture of the mechanically stirred, sparged vessel, the model offers the advantage of considerable mathematical simplicity. The model should be tested more extensively, against other experimental data, to establish the conditions of its validity, but preliminary comparisons with the data on the oxidation of cyclohexane are encouraging and suggest that the phenomenon of interaction between bubbles is not negligible in stirred vessels when the holdup is high and/or the penetration depths are large.

Notation

a = interfacial area per unit volume of dispersion, m^2/m^3
b = outer radius of cell model, m
c_L = concentration of dissolved gas (or oxygen) in bulk liquid, kmol/m^3
c_o = concentration of dissolved gas (or oxygen) at any distance from interface, kmol/m^3
c^* = concentration of dissolved gas (or oxygen) at interface (equilibrium value), kmol/m^3
c^{**} = value of c^* at partial pressure at contactor outlet, if all oxygen entering the reactor were to leave without any being absorbed, kmol/m^3
D = molecular diffusivity of gaseous solute in liquid phase (in particular, of oxygen in cyclohexane), m^2/s
D_p = diffusivity of reaction products in medium of oxidizing cyclohexane, m^2/s
E = enhancement factor
$f(\tau)$ = distribution of internal bubble ages in a well-mixed zone
G_2 = total molar flow rate of gases at outlet of contactor, kmol/s
H = Henry's law coefficient, mol frac/bar
H' = Henry's law coefficient, kmol/(m^3 · bar)
H_G = gas holdup
k = first-order reaction rate constant, s^{-1}
k_{01} = rate constant in expression for cyclohexane conversion rate, s^{-1}
k_{02} = overall rate constant, $m^3/(s \cdot kmol)$
k_L = physical mass transfer coefficient, m · s^{-1}
k_La = volumetric mass transfer coefficient, physical, defined per unit dispersion volume, s^{-1}
K^* = property group, Eq. 28, m · s^{-1}
m = reaction order of a general gas-liquid reaction with respect to gaseous reactant
M = diffusion-reaction parameter, defined for zero-order kinetics of cyclohexane oxidation
M_1 = diffusion-reaction parameter defined for reaction between cyclohexane and oxygen
M_2 = diffusion-reaction parameter defined for reaction between reaction products and oxygen
n = reaction order of a general gas-liquid reaction with respect to liquid phase reactant
N_A = diffusion flux, kmol/(m^2 · s)
N_{A1} = average diffusion flux in zone 1, kmol/(m^2 · s)
p = Laplace parameter, identified with reciprocal of mean residence time in a well-mixed zone, s^{-1}
P_R = reactor pressure, bar
q = dimensionless group D_pc_p/DC^*
q_i = molar flow rate of oxygen into reactor, kmol/s
r = radial distance from center of a bubble, m
r_b = Sauter mean bubble radius, m
r_{bulk} = rate of reaction of oxygen in liquid bulk, kmol/(m^3 · s)
V_{GL} = dispersion volume, m^3
x = distance in liquid from gas-liquid interface, measured along normal to interface, m
z = nondimensional penetration depth in fast reaction regime = x/δ
Z = c_or, transformed variable for concentration of dissolved gas, kmol/m^2
Z_L = $b \cdot c_o(b)$, value of Z at outer radius of model cell, kmol/m^2

Greek letters

δ = film thickness, m
$\theta = z\sqrt{(M_1/q)}$
λ = penetration depth in fast reaction regime, m
ρ_m = molar density of liquid, kmol/m^3
τ = bubble age, s
$\phi = \sqrt{(p + k)}/\sqrt{D}$, m^{-1}
ψ_1 = dimensionless variable, Eq. 33
ψ_2 = dimensionless variable, Eq. 32

Subscripts

o = oxygen
p = product
x = value at a distance x from gas-liquid interface
1 = first-order kinetics in oxygen
0 = initial value
λ = value at a distance λ from gas-liquid interface

Literature Cited

Astarita, G., *Mass Transfer with Chemical Reaction,* Elsevier, Amsterdam (1967).

Carpenter, K. J., "Fluid Processing in Agitated Vessels," *Chem. Eng. Res. Des.*, **64**(1), 3 (1986).

Danckwerts, P. V., *Gas-Liquid Reactions,* McGraw-Hill, New York (1970).

Darde, T., N. Midoux, and J.-C. Charpentier, "Contributions to the Analysis of the Selectivity in Gas-Liquid Reaction. I: Literature and Theory," *Chem. Eng. Commun.*, **22,** 221 (1983).

Flores-Fernandes, G., and R. Mann, "Gas Absorption with Radical Multiplying Chain-type Reaction," *Chem. Eng. Sci.*, **33,** 15454 (1978).

Gal-Or, B., and H. E. Hoelscher, "A Mathematical Treatment of the Effect of Particle Size Distribution on Mass Transfer in Dispersion," *AIChE J.*, **12,** 499 (1966).

Gal-Or, B., and W. Resnick, "Mass Transfer from Gas Bubbles in an Agitated Vessel with and without Simultaneous Chemical Reaction," *Chem. Eng. Sci.*, **19,** 653 (1964).

———, "Gas Residence Time in Agitated Gas-Liquid Contactor," *Ind. Eng. Chem. Process Des. Dev.*, **5**(1), 17 (1966).

Hanhart, J., H. Kramers, and K. R. Westerterp, "The Residence Time Distribution of the Gas in an Agitated Gas-Liquid Contactor," *Chem. Eng. Sci.*, **18,** 503 (1963).

Haynes, H. W., Jr., "Analysis of Slow Gas-Liquid Reactions in Continuous Stirred-Tank Reactors," *Chem. Eng. Commun.*, **23,** 315 (1983).

Hikita, H., and S. Asai, "Gas Absorption with (m, n)th-Order Irreversible Chemical Reaction," *Int. Chem. Eng.*, **4,** 332 (1964).

Mann, R., "Gas-Liquid Stirred Vessel Mixers: Toward a Unified Theory Based on Networks-of-Zones," *Chem. Eng. Res. Des.*, **64**(1), 23 (1986).

Sim, M., and R. Mann, "Gas Absorption with Autocatalytic Reaction," *Chem. Eng. Sci.*, **30,** 1215 (1975).

Sridhar, T., and O. E. Potter, "Predicting Diffusion Coefficients," *AIChE J.*, **23**(4), 590 (1977).

———, "Interfacial Area Measurements in Gas-Liquid Agitated Vessels—Comparison of Techniques," *Chem. Eng. Sci.*, **33,** 1347 (1978).

———, "Gas Holdups and Bubble Diameters in Pressurized Gas-Liquid Stirred Vessels," *Ind. Eng., Chem. Fundam.*, **19,** 21 (1980a).

———, "Interfacial Areas in Gas-Liquid Stirred Vessels," *Chem. Eng. Sci.*, **35,** 683 (1980b).

Suresh, A. K. (Suresh A. Krishnamurthy), "Mass Transfer and Chemical Reaction in Cyclohexane Oxidation," Ph.D. Thesis, Dept. Chem. Eng., Monash Univ., Clayton, Australia (1986).

Suresh, A. K., T. Sridhar, and O. E. Potter, "Mass Transfer and Solubility in Auto-Catalytic Oxidation of Cyclohexane," *AIChE J.*, **33**(12) (Dec., 1987a).

———, "Auto-Catalytic Oxidation of Cyclohexane—Modelling the Reaction Kinetics," *AIChE J.*, **33**(12) (Dec., 1987b).

Manuscript received July 22, 1986, and revision received July 13, 1987.